Biophysical Chemistry 184 (2013) 87–94

Contents lists available at ScienceDirect

Biophysical Chemistry

journal homepage: http://www.elsevier.com/locate/biophyschem

Strategy using three layers of surface charge for computing solvation free energy of ions

Pei-Kun Yang

Department of Biomedical Engineering, I-SHOU University, Kaohsiung 840, Taiwan, ROC

HIGHLIGHTS

- We develop the strategy to compute the solvation free energy.
- The TIP4P water model was incorporated into the continuum solvent model.
- The dielectric polarization calculated from this strategy was similar to from molecular dynamic simulations.
- We derive the analytical solution for the solvation free energy of ions.
- The hydration free energies of various ions calculated from the derived equation were similar to from experimental data.

GRAPHICAL ABSTRACT

The values of ΔG_{hyd}^{cal} (red ×) were calculated using the derived equation with the R_{gmax} of ions and compared with the values from the experiments (black ○).

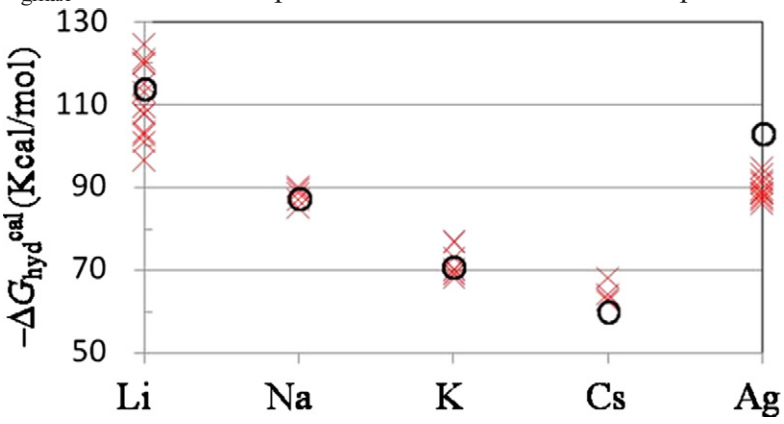

ARTICLE INFO

Article history:
Received 8 September 2013
Received in revised form 26 September 2013
Accepted 29 September 2013
Available online 8 October 2013

Keywords:
Born equation
Continuum solvent model
Surface water
Excluded solvent volume
TIP4P

ABSTRACT

Continuum solvent model is the common used strategy for computing the solvation free energy. However, the dielectric polarization from Gauss's law differs from that obtained from molecular dynamics simulations. To mimic the dielectric polarization surrounding a solute in molecular dynamics simulations, the first-shell water molecule was modeled using a charge distribution of TIP4P molecule in a hard sphere. The dielectric polarization of the first-shell water was modeled as a pair of surface charge layers with a fixed distance between them, but with variable, equal, and opposite charge magnitudes that respond to the electric field on the first-shell water. The water outside the first shell water is treated as a bulk solvent, and the electric effect of the bulk solvent can be modeled as a surface charge. Based on this strategy, the analytical solution describing the solvation free energy of ions was derived, and the values of computed solvation free energy were compared to the values of experiments.

1. Introduction

Solvent plays a significant role in the stability of protein conformations [1] and the binding affinity of protein–protein/ligand interactions [2]. A lot of strategies had been developed for computing solvation free energy. They can be grouped into explicit [3], hybrid [4,5] and implicit [6,7] solvent models. Several of these strategies, such as the Born equation [8], the generalized Born equation [9], Poisson's equation [10], the two Born radii [11,12], the Poisson–Boltzmann equation, and the distance-dependent dielectric constant were derived from continuum solvent models. The continuum solvent model is conventionally incorporated

E-mail address: peikun@isu.edu.tw.

0301-4622/$ – see front matter
http://dx.doi.org/10.1016/j.bpc.2013.09.007

into the quantum mechanism to examine protein functions [7] or incorporated into docking algorithms for computer-aided drug design [13,14].

The solvation free energy ΔG^{cal}_{hyd} can be partitioned into the charging solvation free energy and nonpolar free energy [15]. The charging solvation free energy $\Delta G_{elec}(0 \rightarrow Q)$ can be calculated by integration of the electrostatic potential $\Phi(q)$ at the solute, which is contributed by the solvent for the solute charge to increase from 0 to Q [8]. The nonpolar free energy ΔG_{np} depends on the solute surface area and can be approximated as $\Delta G_{np} = \gamma A + \beta$, where $A(Å^2)$ is the solute surface area, the parameter $\gamma = 0.00542$ kcal/(mol·Å^2), and $\beta = 0.92$ kcal/mol [16]. Therefore, the ΔG^{cal}_{hyd} is

$$\Delta G^{cal}_{hyd} = \int_0^Q \Phi(q)dq + (\gamma A + \beta). \quad (1)$$

The $\Phi(q)$ can be calculated from the dielectric polarization, $-P$, based on the continuum solvent model. However, the $P(r)$ from molecular dynamics (MD) simulations behaves oscillation as distance r from the solute. This substantially differs from the P proposed in the continuum solvent model [17–19]. Despite this difference, the parameters, Born radii, are used to fit the experimental solvation free energy. A solute comprising n atoms contains n Born radii and only one experimental solvation free energy. From this perspective, numerous sets of Born radii can be adjusted to fit the experimental solvation free energy. The experimental data of solvation free energy is integrated and weighted by the probability over all possible solute conformations. However, the n parameters of the Born radii are insufficient for fitting the solvation free energy from numerous solute conformations unless the function describing the solvation free energy is accurate [11].

Therefore, the solvent scheme developed in this study mimics the P from MD simulations. It was known that to treat a solvent molecule as a point dipole at the center of a hard sphere, and to assume the electric dipole per water molecule, $p(r)$, is proportional to the electric field, the solution of the $p(r)$ exhibits oscillations as distance r from the solute as observed from MD simulations [11,19,20]. Therefore, in this study, the surface water molecule was modeled using a TIP4P charge distribution in a hard sphere solvent [21,22], and the water molecules outside the first-shell water were treated as a bulk solvent. The electric effect of the bulk solvent can be solved by Maxwell's equations by treating the water as the dielectric continuum, and the dielectric polarization of the bulk solvent can be modeled as a surface charge [23]. The dielectric polarization of the first-shell water is proportional to the electric field that is contributed from the solute and the excluded solvent molecules. The electric effect of the first-shell dielectric polarization is modeled as a pair of surface charge layers with a fixed distance between them, but with variable, equal, and opposite charge magnitudes that respond to the electric field. For one-particle solute, the equation describing the solvation free energy was derived by this solvent scheme, and the solvation free energies of ions calculated using the derived equation were compared with the experimental data.

2. Methods

2.1. MD simulations

The solute with charge $Q = -1.0$ e, -0.8 e, -0.4 e, $+0.4$ e, $+0.8$ e, or $+1.0$ e was fixed at the center of a spherical water cluster with a radius of 15 Å containing 471 TIP3P [21] water molecules. The vdW parameters of the solutes were assigned the same values as the oxygen atoms of the TIP3P water, where $\varepsilon = -0.1521$ kcal/mol and $R_{min}/2 = 1.7682$ Å. Simulations were performed in an NVE ensemble by using the CHARMM package [24] and applying spherical boundary conditions without cutoffs. The ion–water and water–water interaction energies were calculated by summing the electrostatic and vdW pairwise energies. The length of the O–H bonds in TIP3P and the angle of the H–O–H bond were constrained during the simulations by using the SHAKE algorithm [25]. All atoms were propagated according to Newton's equations by using the leapfrog Verlet algorithm and a time step of 2 *fs* at a mean temperature of 300 K. Each system was first minimized for 1000 steps, equilibrated for 100 *ps*, and then subjected to 4 *ns* of production dynamics for analysis.

2.2. Calculating the normalized dielectric polarization $P_n(r)$ from the trajectories of MD simulations

The $P_n(r)$ is defined as $4\pi r^2 P(r)/Q$. The amplitude of $P_n(r)$ can be calculated by summing the radial direction of the electric dipole moment of the water molecules with its oxygen atom located between $r - \Delta r/2$ and $r + \Delta r/2$ over N_C configurations, divided by the solute charge Q as,

$$P_n(r) = \frac{1}{QN_C\Delta r}\int_{r-\Delta r/2}^{r+\Delta r/2}\sum_{l=1}^{N_c}\sum_{m=1}^{n}\sum_{i=1}^{3} q_i\left(\mathbf{r}_i^{lm}\bullet\frac{\mathbf{r}_O^{lm}}{r_O^{lm}}\right)\delta\left(r'-r_O^{lm}\right)dr' \quad (2)$$

where the first summation is over N_c configurations and the second summation is over n solvent molecules in the simulation system, where r_O^{lm} denotes the oxygen atom coordinates for the water molecule m in the configuration l, r_i^{lm} denotes the coordinates of atom i of water molecules m in configuration l, q_i is the charge of water atom i, Q is the solute charge, and Δr is set as 0.1 Å.

3. Theory

For a solute molecule in a macroscopic water cluster, the solvent dielectric polarization changes drastically in the near-solute and water/air interface regions, and approaches those of the bulk solvent in the intermediate region. For the solvent molecules in the intermediate region, the electric effect of the solvent can be modeled as a continuum solvent and solved by Gauss's law [23]. For the solvent in the water/air interface region, the solvent dielectric polarization is independent on the distribution of the solute charge, and the electrostatic potential at the solute contributed by the solvent in the water/air interface region is constant [26–28]. Hence, $\Phi(q)$ in Eq. (1) can be computed by summing $\Phi_{struc}(q)$, $\Phi_{con}(q)$, and Φ_{sur} as $\Phi(q) = \Phi_{struc}(q) + \Phi_{con}(q) + \Phi_{sur}$, [26] where $\Phi_{struc}(q)$, $\Phi_{con}(q)$, and Φ_{sur} are contributed by the water cluster in the near solute, the bulk solvent, and the water/air interface region, respectively. By substituting it into Eq. (1), ΔG^{cal}_{hyd} can be calculated as,

$$\Delta G^{cal}_{hyd} = \int_0^Q \Phi_{struc}(q)dq + \int_0^Q \Phi_{con}(q)dq + Q\Phi_{sur} + (\gamma A + \beta). \quad (3)$$

In Eq. (3), $A(Å^2)$ is the solute surface area, the parameter $\gamma = 0.00542$ kcal/(mol·Å^2), and$\beta = 0.92$ kcal/mol [16]. For the ion with a charge $Q = -1.0$ e, -0.8 e, -0.4 e, $+0.4$ e, $+0.8$ e, or $+1.0$ e in TIP3P water, the $P_n(r)$ calculated using Eq. (2) has a large peak at the position near R_{gmax} according to MD simulations and approaches a constant value in the region far away from the solute (Fig. 1), where R_{gmax} is the first peak position in the ion-water radial distribution function. For mimicking the P observed in MD simulations, the solvent scheme used in this study was the surface water at the position distance solute R_{gmax} and the continuum solvent model used in the region distance solute greater than $(R_{gmax} + R_W)$, where R_W is the water molecule radius (Fig. 1). In Eq. (3), $\Phi_{con}(q)$ is contributed by the continuum solvent outside the first-shell water and is in the solute distance region greater than $(R_{gmax} + R_W)$. $\Delta_{con}(q)$ can be calculated as

$$\Phi_{con}(q) = -\frac{q(1-1/\varepsilon_r)}{4\pi\varepsilon_0\left(R_{gmax} + R_W\right)} \quad (4)$$

$\Phi_{struc}(q)$ was computed by incorporating TIP4P water model. The TIP4P model has four interaction sites. The three sites are on the three atoms, and the fourth site is moved off the oxygen and towards the hydrogens

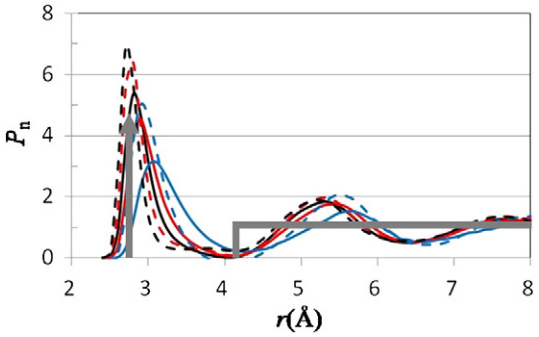

Fig. 1. Comparison of $P_n(r)$ values obtained from the MD simulations and the solvent scheme used in this study. The solute with the charge $Q = -1.0$ e (dashed black), -0.8 e (dashed red), -0.4 e (dashed blue), $+0.4$ e (solid blue), $+0.8$ e (solid red), or $+1.0$ e (solid black) was in the TIP3P water cluster, and the water molecule trajectories are obtained after equilibrium. The $P_n(r)$ was calculated using Eq. (2). The results show that the $P_n(r)$ from MD simulations has a large peak in the first-shell water region and approaches a constant value in the region far from the solute. For the solvent scheme used in this study, the water in the first shell is modeled as surface water at the position $r = R_{gmax}$, and a continuum solvent model is used in the region $r \geq (R_{gmax} + R_W)$ (gray line). The dielectric polarization of the surface water was described using Dirac delta function, and the dielectric polarization in the continuum solvent region was described using Heaviside function.

at a point (M) on the bisector of the HOH angle. The M site with charge q_M is displaced at 0.15 Å from the oxygen atom. Charges of the two hydrogen atoms were q_{H1} and q_{H2}, and a Lennard–Jones sphere is placed on the oxygen atom [21,22]. Treating the electric effect of surface waters as two layers of surface charge density, the negative and positive surface charge densities are from the M site and hydrogen atoms of the TIP4P water model, and are at the solute distance positions $(R_{gmax} + s(E_{net})r_{M,O})$ and $(R_{gmax} + s(E_{net})r_{Hb,O})$, respectively, where $s(E_{net})$ is the sign of the net electric field on the surface water, $r_{M,O}$ and $r_{Hb,O}$ are the distance between the oxygen atom and the M site and hydrogen bisector center of the TIP4P, respectively. The amplitude of the surface charge density depends on E_{net} on the surface water. After evaluating the amplitude of the positive and negative surface charge density, the equations describing $\Phi_{struc}(q)$ in Eq. (3) and the solvation free energy can be derived.

The dielectric polarization P is decomposed into the product of the electric dipole moment per water molecule p, the bulk solvent molecular density N_{bulk}, and the ratio between the solvent molecular density and the bulk solvent molecular density g, as $P(r) = N_{bulk}g(r)p(r)$ [17,19]. p is proportional to the electric field at the solvent molecule E_{net} [17,18] when $p(r) = \varepsilon_0\gamma_{mol}E_{net}(r)$, where ε_0 is the vacuum permittivity, and γ_{mol} is the solvent molecular polarizability. Combining these relations, $P(r)$ can be written as

$$\mathbf{P}(\mathbf{r}) = N_{bulk}g(\mathbf{r})\varepsilon_0\gamma_{mol}\mathbf{E}_{net}(\mathbf{r}). \quad (5)$$

The E_{net} can be decomposed into contributed from the solute, $-E_{solute}$, and the other solvent, $-E_{solvent}$. For one-particle solute with a charge Q in the water solvent, and one of the solvent molecules at position $(x = 0, y = 0, z)$, the amplitude of $E_{solvent}(z)$ can be calculated as an integration of $E_{solvent}(z; R)$ as,

$$E_{solvent}(z) = \int_0^\infty E_{solvent}(z;R)dR \quad (6)$$

where $E_{solvent}(z; R)$ is the electrostatic field at $(0, 0, z)$ from the dielectric polarization $P(R)$.

For the TIP4P water model, the electric effect of the $P(R)$ was modeled as the negative surface charge density with amplitude of $-|P(R)|/(r_{Hb,O} - r_{M,O})$ at distance R_- from the solute, and the positive surface charge density with amplitudeof $+|P(R)|/(r_{Hb,O} - r_{M,O})$ at distance R_+ from the solute. $(r_{Hb,O} - r_{M,O})$ is the distance between the M site and the hydrogen bisector center of the TIP4P molecule. Assuming that the radius of water molecule is R_W, $E_{solvent}(z; R)$ can be calculated as (Fig. 2),

$$E_{solvent}(z;R) = \frac{|P(R)|}{4\pi\varepsilon_0\left(r_{Hb,O}-r_{M,O}\right)}\int_{\theta_W}^{\pi}\left[\frac{z-R_+\cos\theta}{\left(R_+^2+z^2-2R_+z\cos\theta\right)^{3/2}} - \frac{z-R_-\cos\theta}{\left(R_-^2+z^2-2R_-z\cos\theta\right)^{3/2}}\right]2\pi R^2\sin\theta d\theta. \quad (7)$$

In Eq. (7), $\cos\theta_W = (z^2 + R^2 - R_W^2)/(2zR)$.

By integrating the electrostatic field on the right side of Eq. (7), $E_{solvent}(z; R)$ is,

$$E_{solvent}(z;R) = \frac{R^{3/2}|P(R)|}{4\varepsilon_0\left(r_{Hb,O}-r_{M,O}\right)z^2}\left[\frac{z^2+R^2-2RR_+-R_W^2}{\sqrt{\left(z^2-R_+R\right)\left(R-R_+\right)+R_+R_W^2}} - \frac{z^2+R^2-2RR_--R_W^2}{\sqrt{\left(z^2-R_-R\right)\left(R-R_-\right)+R_-R_W^2}}\right]. \quad (8)$$

Substitute $R_- = (R + s(E_{net})r_{M,O})$ and $R_+ = (R + s(E_{net})r_{Hb,O})$ into (8), $E_{solvent}(z; R)$ is,

$$E_{solvent}(z;R) = \frac{R|P(R)|}{4\varepsilon_0\left(r_{Hb,O}-r_{M,O}\right)R_Wz^2}\left[\frac{z^2-R^2-2Rs(E_{net})r_{Hb,O}-R_W^2}{\sqrt{1+\frac{r_{Hb,O}}{R_W^2}\left(r_{Hb,O}+s(E_{net})\frac{R_W^2-z^2+R^2}{R}\right)}} - \frac{z^2-R^2-2Rs(E_{net})r_{M,O}-R_W^2}{\sqrt{1+\frac{r_{M,O}}{R_W^2}\left(r_{M,O}+s(E_{net})\frac{R_W^2-z^2+R^2}{R}\right)}}\right]. \quad (9)$$

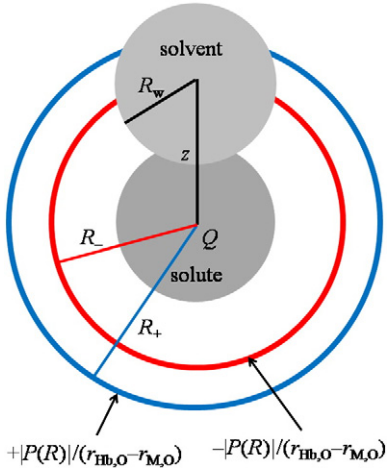

Fig. 2. Calculation of $E_{solvent}(z)$. For the solute with a charge Q at the origin, one of the solvent molecules with a radius R_W is located at the position of $(x = 0, y = 0, z)$. The electrostatic field at $(0, 0, z)$ contributed by the dielectric polarization $P(R)$ is calculated by summing the positive surface charge density at R_+ with amplitude of $+|P(R)|/(r_{Hb,O} - r_{M,O})$ and the negative surface charge density at R_- with amplitude of $-|P(R)|/(r_{Hb,O} - r_{M,O})$. The distance between R_+ and R_- is $(r_{Hb,O} - r_{M,O})$.

$E_{solvent}(z)$ can be calculated using Eq. (6) as

$$E_{solvent}(z) = \int_0^{z-Rw} E_{solvent}(z;R)dR + \int_{z-Rw}^{z+Rw} E_{solvent}(z;R)dR + \int_{z+Rw}^{\infty} E_{solvent}(z;R)dR. \quad (10)$$

The first and third terms on the right side of Eq. (10) are zero based on Gauss's law.

The electric effect of $P((z-R_W)<R<(z+R_W))$ on the solute is mimicked using the surface dielectric polarization $P_S(z)$. $P_S(z)$ is approximated as

$$P_S(z) = \int_{z-R_W}^{z+R_W} P(R)dR. \quad (11)$$

By substituting Eqs. (9) and (11) into Eq. (10), $E_{solvent}(R_{gmax})$ can be approximated as,

$$E_{solvent}\left(R_{gmax}\right) = -\frac{P_S\left(R_{gmax}\right)}{4\varepsilon_0\left(r_{Hb,O}-r_{M,O}\right)R_W R_{gmax}}\left[\frac{2r_{Hb,O}R_{gmax}+s(E_{net})R_W^2}{\sqrt{1+\frac{r_{Hb,O}}{R_W^2}\left(r_{Hb,O}+s(E_{net})\frac{R_W^2}{R_{gmax}}\right)}} - \frac{2r_{M,O}R_{gmax}+s(E_{net})R_W^2}{\sqrt{1+\frac{r_{M,O}}{R_W^2}\left(r_{M,O}+s(E_{net})\frac{R_W^2}{R_{gmax}}\right)}}\right]. \quad (12)$$

By substituting Eqs. (5) into (11) and treating $g(r)=1$, $P_S(R_{gmax})$ can be approximated as

$$P_S\left(R_{gmax}\right) \approx 2R_W N_{bulk}\varepsilon_0\gamma_{mol}E_{net}\left(R_{gmax}\right). \quad (13)$$

The $E_{net}(R_{gmax})$ in Eq. (13) is a summation of $E_{solute}(R_{gmax})$ and $E_{solvent}(R_{gmax})$. By substituting Eqs. (13) into (12),

$$\frac{P_S\left(R_{gmax}\right)}{2R_W N_{bulk}\varepsilon_0\gamma_{mol}} = \frac{Q}{4\pi\varepsilon_0 R_{g\,max}^2} - \frac{P_S\left(R_{gmax}\right)}{4\varepsilon_0\left(r_{Hb,O}-r_{M,O}\right)R_W R_{gmax}}\left[\frac{2r_{Hb,O}R_{gmax}+s(E_{net})R_W^2}{\sqrt{1+\frac{r_{Hb,O}}{R_W^2}\left(r_{Hb,O}+s(E_{net})\frac{R_W^2}{R_{gmax}}\right)}} - \frac{2r_{M,O}R_{gmax}+s(E_{net})R_W^2}{\sqrt{1+\frac{r_{M,O}}{R_W^2}\left(r_{M,O}+s(E_{net})\frac{R_W^2}{R_{gmax}}\right)}}\right]. \quad (14)$$

P_S can be solved as

$$4\pi R_{gmax}^2 P_S\left(R_{gmax}\right) = 2R_W CQ \quad (15)$$

where

$$\frac{1}{C} = \frac{1}{2\left(r_{Hb,O}-r_{M,O}\right)R_{gmax}}\left[\frac{2r_{Hb,O}R_{gmax}+s(E_{net})R_W^2}{\sqrt{1+\frac{r_{Hb,O}}{R_W^2}\left(r_{Hb,O}+s(E_{net})\frac{R_W^2}{R_{gmax}}\right)}} - \frac{2r_{M,O}R_{gmax}+s(E_{net})R_W^2}{\sqrt{1+\frac{r_{M,O}}{R_W^2}\left(r_{M,O}+s(E_{net})\frac{R_W^2}{R_{gmax}}\right)}}\right] + \frac{1}{N_{bulk}\gamma_{mol}}. \quad (16)$$

The electric potential at the solute contributed by the surface dielectric polarization at distance $r = R_{gmax}$ from the solute, $-\Phi_{struc}(q)$,is

$$\Phi_{struc}(q) = \frac{\frac{1}{4\pi\varepsilon_0}\left[4\pi R_{gmax}^2\left|P_S\left(R_{gmax}\right)\right|/\left(r_{Hb,O}-r_{M,O}\right)\right.}{R_{gmax}+s(E_{net})r_{Hb,O}} \left. - \frac{4\pi R_{gmax}^2\left|P_S\left(R_{gmax}\right)\right|/\left(r_{Hb,O}-r_{M,O}\right)}{R_{gmax}+s(E_{net})r_{M,O}}\right]. \quad (17)$$

By substituting Eqs. (15) into (17), $\Phi_{struc}(q)$ is

$$\Phi_{struc}(q) = -\frac{R_W CQ}{2\pi\varepsilon_0\left[R_{gmax}+s(E_{net})r_{Hb,O}\right]\left[R_{gmax}+s(E_{net})r_{M,O}\right]}. \quad (18)$$

By substituting Eqs. (4) and (18) into (3), ΔG_{hyd}^{cal} is

$$\Delta G_{hyd}^{cal} = Q\Phi_{sur} + (\gamma A+\beta) - \frac{Q^2}{8\pi\varepsilon_0}\left\{\frac{2R_W C}{\left[R_{gmax}+s(E_{net})r_{Hb,O}\right]\left[R_{gmax}+s(E_{net})r_{M,O}\right]} + \frac{1-1/\varepsilon_r}{R_{gmax}+R_W}\right\}. \quad (19)$$

In (19), Q is the solute charge, Φ_{sur} is not considered and set to be zero, $A(Å^2)$ is the solute surface area, the parameter $\gamma = 0.00542$ kcal/(mol·Å^2), $\beta = 0.92$ kcal/mol are from Ooi [16], $r_{Hb,O}$ and $r_{M,O}$ are from TIP4P water model [21,22], R_W from the pair distribution functions of liquid water at 25 °C is 1.4 Å [29], ε_r of water solvent is 80, and C was calculated using Eq. (16).

4. Results

4.1. Developing the solvent scheme for computing the solvation free energy

To treat the electric effect of the solvent as the dielectric continuum and solve the electric potential at the solute using Poisson's equation is the conventional used strategy to calculate the solvation free energy. However, the P in the near-solute region solved from the continuum solvent model differs in observations of MD simulations [20,30]. It was known that by treating the first-shell water as a point dipole in a hard sphere, assuming that the P is proportional to $E_{net}(r)$, the calculated $P(r)$ can show that the oscillation decay depends on the distance r from the solute, as observed in the MD simulations. Therefore, in this project, the first-shell water molecule was treated as the charge distribution of TIP4P in a hard sphere, and the water molecules outside the first-shell water were treated as dielectric continuum. The dielectric polarization of the first-shell water is modeled as a pair of surface charge layers with a fixed distance between them, but with variable charge magnitudes that respond to the electric field on the first-shell water. The intermediate water is treated as a bulk solvent. This strategy was developed for the solute with multiple atoms. For one-particle solute, the analytical solution describing the solvation free energy was derived.

4.2. The solvation free energies of ions contributed by the first-shell water are similar to those from the continuum solvent region

For univalent cations, divalent cations, trivalent cations, tetravalent cations, and univalent anions, the solvation free energies were calculated using Eq. (19). The percentages of the ΔG_{hyd}^{cal} contributed by the first-shell water, the continuum solvent region, and the non-polar free energy are approximately 54.4%, 46.2%, and 0.6%, respectively (Table 1), which indicate the significance of accurately estimating the solvation free energy contributed by the first-shell water.

4.3. Comparison of the solvation free energy calculated using Eq. (19), the original Born model and from the experiments

The equation describing the solvation free energy according to the original Born model is $\Delta G_{Born} = -Q^2(1-1/\varepsilon_r)/(8\pi\varepsilon_0 R_{ion})$. Assuming that $R_{ion} = R_{gmax} - R_W$, the dependencies of ΔG_{Born} and ΔG_{hyd}^{cal} on R_{gmax} were plotted in Table 1 and Fig. 3. The R_W from the pair distribution functions of liquid water at 25 °C is 1.4 Å [29]. However, the water in the first hydration shell of an ion is under much stronger forces than those due to the fields prevailing in liquid water, the R_W is estimated at 1.39 Å [31,32]. The results show that the solvation free energy calculated using the solvent scheme developed in this study was much more accurate than that of ΔG_{Born} for univalent cations, divalent cations, trivalent cations, and tetravalent cations.

4.4. Comparison of $-\Delta G_{hyd}^{cal}$ and $-\Delta G_{exp}$ values for various ions

The solvation free energies calculated using Eq. (19) were compared with the solvation free energies from the experiments [33]. For Li^+, Na^+ and K^+, the values of $-\Delta G_{exp}$ were in the distribution region of the $-\Delta G_{hyd}^{cal}$ values (Fig. 4a). For Cs^+, the $-\Delta G_{hyd}^{cal}$ value was

Table 1
Comparison of the solvation free energies of ions calculated using Eq. (19) the experimental data.

	Q[a]	R_{gmax}[b]	$-\Delta G_{exp}$[c]	ΔG_{np}[d]	$-\Delta G_{con}$[e]	$-\Delta G_{struc}$[f]	$-\Delta G_{hyd}^{cal}$[g]	E_{rr}%[h]	$-\Delta G_{Born}$[i]
Li	1	1.95	113.6	1.4	48.9	72.2	119.8	5.4	292.7
Ag	1	2.43	102.9	1.6	42.8	47.1	88.3	−14.2	157.6
Na	1	2.46	87.3	1.6	42.5	46.0	86.8	−0.6	153.2
K	1	2.80	70.6	1.8	39.0	35.8	73.1	3.5	116.3
Cs	1	2.95	59.8	1.8	37.7	32.3	68.2	14.0	105.1
Be	2	1.67	573.0	1.3	213.6	392.0	604.3	5.5	2341.8
Zn	2	2.04	467.7	1.4	190.6	264.5	453.7	−3.0	1008.8
Ni	2	2.04	473.7	1.4	190.6	264.5	453.7	−4.2	1008.8
Cu	2	2.05	480.9	1.4	190.1	262.0	450.6	−6.3	993.5
Co	2	2.08	458.1	1.4	188.4	254.7	441.7	−3.6	950.3
Mg	2	2.12	437.8	1.5	186.3	245.4	430.2	−1.7	898.2
Fe	2	2.12	440.2	1.5	186.3	245.4	430.2	−2.3	898.2
Mn	2	2.20	421.1	1.5	182.1	228.4	409.0	−2.9	809.5
Cd	2	2.31	419.9	1.5	176.7	207.7	382.9	−8.8	712.7
Sn	2	2.34	328.9	1.5	175.3	202.6	376.3	14.4	690.2
Hg	2	2.41	421.1	1.6	172.1	192.9	361.8	1.1	649.2
Ca	2	2.40	360.0	1.6	172.6	191.3	363.8	−14.1	642.8
Ca	2	2.44	360.0	1.6	170.8	186.8	355.9	−1.1	624.5
Ca	2	2.46	360.0	1.6	169.9	183.8	352.1	−2.2	612.8
Sr	2	2.64	330.1	1.7	162.3	160.4	321.0	−2.8	524.6
Ba	2	2.90	299.0	1.8	152.5	133.7	284.4	−4.9	434.2
Al	3	1.87	1082.5	1.4	451.2	705.7	1155.5	6.7	3073.6
Cr	3	1.95	959.3	1.4	440.4	650.1	1089.0	13.5	2634.5
Cr	3	1.97	959.3	1.4	437.8	637.2	1073.6	11.9	2543.7
Cr	3	2.00	959.3	1.4	434.3	620.5	1053.4	9.8	2430.5
Fe	3	2.01	1020.3	1.4	432.6	612.7	1043.9	2.3	2379.6
In	3	2.15	952.2	1.5	415.6	537.3	951.4	−0.1	1941.2
Tl	3	2.24	949.8	1.5	405.8	497.8	902.1	−5.0	1743.9
Tm	3	2.33	840.9	1.5	395.5	459.6	853.6	1.5	1569.5
Lu	3	2.34	840.9	1.5	394.5	455.8	848.7	0.9	1553.0
Y	3	2.36	825.4	1.6	392.4	448.3	839.1	1.7	1521.0
Er	3	2.36	836.1	1.6	392.4	448.3	839.1	0.4	1521.0
Gd	3	2.37	807.4	1.6	391.3	444.7	834.4	3.3	1505.4
Dy	3	2.39	819.4	1.6	389.3	437.5	825.2	0.7	1475.3
Tb	3	2.40	813.4	1.6	388.2	433.9	820.6	0.9	1460.7
Eu	3	2.45	803.8	1.6	383.2	416.9	798.5	−0.7	1391.8
Sm	3	2.47	795.5	1.6	381.2	410.4	790.0	−0.7	1366.0
Nd	3	2.51	784.7	1.6	377.3	397.8	773.5	−1.4	1317.3
Pr	3	2.54	776.3	1.6	374.4	388.8	761.6	−1.9	1282.9
La	3	2.58	752.4	1.7	370.7	377.2	746.2	−0.8	1239.8
Th	4	2.45	1391.1	1.6	681.2	741.2	1420.9	2.1	2474.3
Th	4	2.49	1391.1	1.6	674.9	720.6	1393.9	0.2	2393.1
F	−1	2.69	111.2	1.7	40.1	54.1	92.5	−16.8	126.1
Br	−1	3.2	75.4	2.0	35.6	36.6	70.3	−6.8	90.6
I	−1	3.58	65.8	2.2	32.9	28.6	59.3	−9.9	74.9

[a] Q(e) is the charge of ions.
[b] R_{gmax}(Å) is the first peak position in the ion–water radial distribution function [34].
[c] ΔG_{exp}(kcal/mol) is the solvation free energy from experiments [33].
[d] ΔG_{np}(kcal/mol) is the nonpolar free energy.
[e] ΔG_{con}(kcal/mol) is the solvation free energy contributed by the continuum solvent region.
[f] ΔG_{struc}(kcal/mol) is the solvation free energy contributed by the first-shell solvent region.
[g] ΔG_{hyd}^{cal}(kcal/mol) is the solvation free energy calculated using Eq. (19). The N_{bulk}, R_W, γ_{mol}, and ε_r used in Eq. (19) were 0.0334/Å^3, 1.4 Å, 51 Å^3 and 80 respectively. The $r_{Hb,O}$ and $r_{M,O}$ used in Eq. (19) were 0.59 Å, and 0.15 Å, respectively. Φ_{sur} in Eq. (19) was set as 0.
[h] $E_{rr}\% = 100(\Delta G_{hyd}^{cal} - \Delta G_{exp})/\Delta G_{exp}$.
[i] ΔG_{Born}(kcal/mol) is the solvation free energy calculated using Born model.

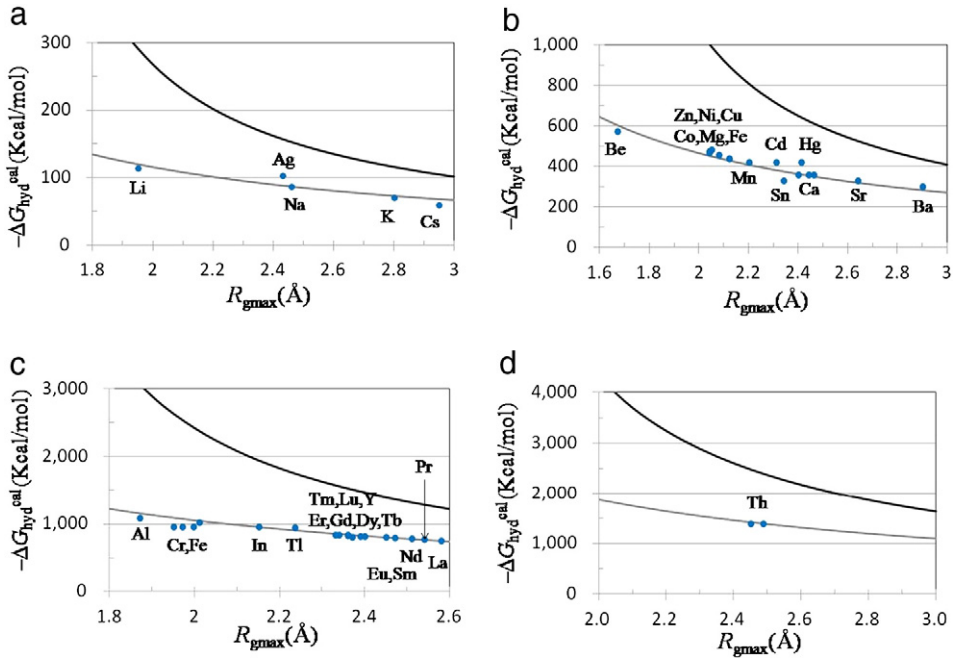

Fig. 3. Dependence of the ΔG_{hyd}^{cal}, ΔG_{Born}, and ΔG_{exp} values of ions on R_{gmax}. For the ions with (a) univalent cations, (b) divalent cations, (C) trivalent cations, and (d) tetravalent cations, the values of ΔG_{hyd}^{cal}(solid gray) and ΔG_{Born}(solid black) were calculated using Eq. (19) and the Born equation, respectively. The ΔG_{exp}(blue ●) was obtained from Table 1. The ionic radius used in the Born equation is estimated by subtracting 1.39 Å from R_{gmax} [31,32].

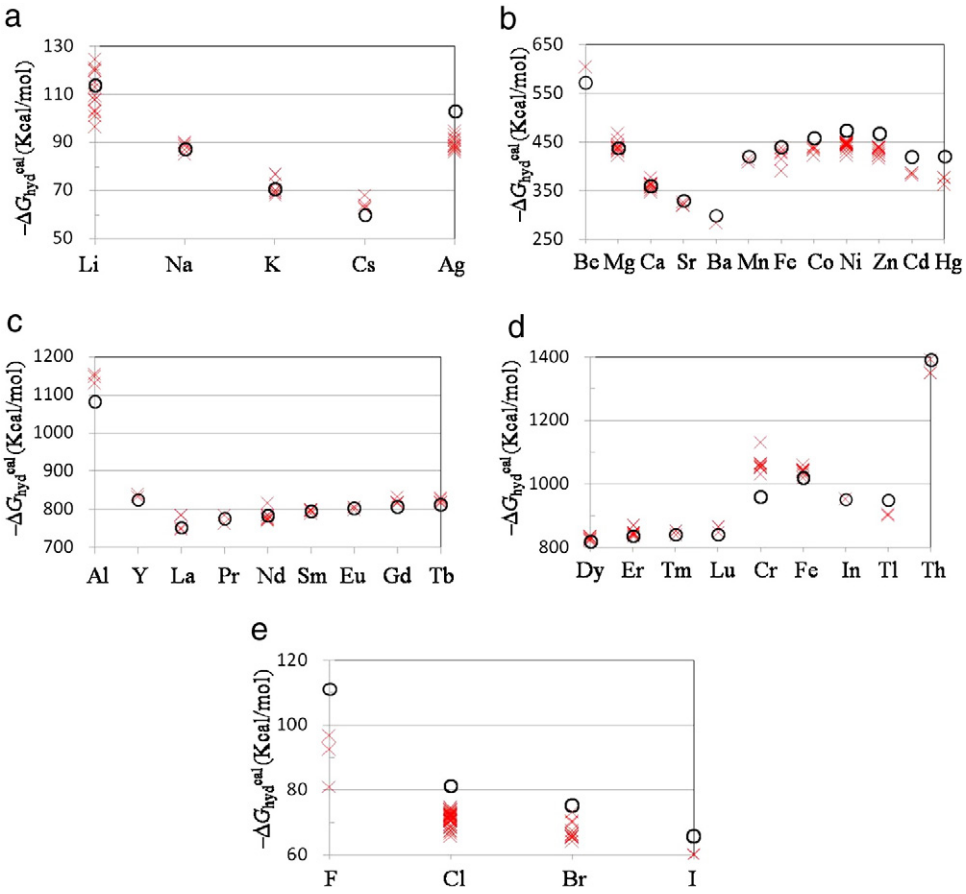

Fig. 4. Comparing the ΔG_{hyd}^{cal} values and the various ion experiments. The values of ΔG_{hyd}^{cal} (red ×) were calculated using R_{gmax} of ions from Ohtaki [35] and compared with the values from the experiments [33] (black ○). Each ion has several structural parameters of the hydration shell of derived from X-ray diffraction and the extended X-ray absorption fine structure method. The ion charges were (a) +1 e, (b) +2 e, (c) +3 e, (d) +3/+4 e, and (e) −1 e, respectively.

slightly higher than that of $-\Delta G_{exp}$(Fig. 4a). For Ag^{+}, the $-\Delta G^{cal}_{hyd}$ value was slightly lower than that of the $-\Delta G_{exp}$(Fig. 4a). For Mg^{++}, Ca^{++}, Sr^{++}, Mn^{++} and Fe^{++}, the $-\Delta G_{exp}$ values were in the region of the $-\Delta G^{cal}_{hyd}$ values (Fig. 4b). For Ba^{++}, Co^{++}, Ni^{++}, Zn^{++}, Cd^{++} and Hg^{++}, the $-\Delta G^{cal}_{hyd}$ values were slightly lower than that of the $-\Delta G_{exp}$ values (Fig. 4b). For Be^{++}, the $-\Delta G^{cal}_{hyd}$ value was slightly higher than that of the $-\Delta G_{exp}$ value (Fig. 4b). For Al^{3+}, the $-\Delta G^{cal}_{hyd}$ value was higher than that of the $-\Delta G_{exp}$ value (Fig. 4c). For Y^{3+}, La^{3+}, Pr^{3+}, Nd^{3+}, Sm^{3+}, Eu^{3+}, Gd^{3+}, and Tb^{3+}, the $-\Delta G_{exp}$ values were in the distribution region of the $-\Delta G^{cal}_{hyd}$ values (Fig. 4c). For Dy^{3+}, Er^{3+}, Tm^{3+}, Lu^{3+}, Fe^{3+}, In^{3+} and Th^{4+}, the $-\Delta G_{exp}$ values were in the distribution region of $-\Delta G^{cal}_{hyd}$ (Fig. 4d). For Cr^{3+}, the $-\Delta G^{cal}_{hyd}$ value was higher than that of the $-\Delta G_{exp}$ value (Fig. 4d). For Tl^{3+}, the $-\Delta G^{cal}_{hyd}$ value was lower than that of the $-\Delta G_{exp}$ value (Fig. 4d). For F^{-}, Cl^{-}, Br^{-}, and I^{-}, the $-\Delta G_{exp}$ values were lower than that of the $-\Delta G^{cal}_{hyd}$ values (Fig. 4e).

5. Discussion

5.1. The parameters used in the derived equation for charging hydration free energy are not from fitting the solvation free energy

The solvent molecular polarizability, $-\gamma_{mol}$, the radius of the water molecule, R_W, and the solvent model are necessary for computing solvation free energy in Eq. (19). The first-shell water molecule was modeled as the charge distribution of TIP4P in a hard sphere. The values of γ_{mol} and R_W are not derived from fitting the solvation free energy. According to the MD simulations, γ_{mol} was 51 Å^3 [18], and, according to neutron diffraction, the R_W from the first peak of the pair distribution function of the oxygen–oxygen atom of liquid water was 1.4 Å [29]. The values of R_{gmax} were from the experiments. Those parameters are not from fitting the solvation free energy.

5.2. $R_{gmax}(q)$ differs compared to and $R_{gmax}(Q)$

For the solute with a charge Q, $R_{gmax}(q)$ is required to compute the charging hydration free energy in Eq. (3), where q is between zero and Q. $R_{gmax}(q)$ decreased as $|q|$ increased. To derive Eq. (19), $R_{gmax}(q)$ was approximated as $R_{gmax}(Q)$. Hence, the $-\Delta G^{cal}_{hyd}$ of the ions calculated using Eq. (19) was overestimated compared to the $-\Delta G_{exp}$ of the ions by considering this error. This can be contrasted to the $-\Delta G^{cal}_{hyd}$ values, which were slightly lower than that of the $-\Delta G_{exp}$ value for the divalent cations (Fig. 4b), and slightly higher than that of the $-\Delta G_{exp}$ value for the trivalent cations (Fig. 4c–d).

5.3. Dielectric saturation

The γ_{mol} used in Eq. (19) was assumed to be constant. γ_{mol} is decreased for the large net electric field on the solvent. Assuming that γ_{mol} is constant, the $-\Delta G^{cal}_{hyd}$ values were slightly higher than that of the $-\Delta G_{exp}$ value for the trivalent cations (Fig. 4c–d). This can be contrasted to the $-\Delta G^{cal}_{hyd}$ values, which were slightly lower than that of the $-\Delta G_{exp}$ values for the univalent and divalent cations (Fig. 4a–b).

5.4. The difference between $-\Delta G^{cal}_{hyd}$ and $-\Delta G_{exp}$ for halide ions

For the halide ions in water, one of the hydrogen atoms of water molecule tends toward an anion. In this project, we assume the net dipole of water molecule tends toward an anion. Therefore, the values of $-\Delta G^{cal}_{hyd}$ were different with the values of $-\Delta G_{exp}$ for halide ions.

5.5. The values of ΔG^{cal}_{hyd} spread around the values calculated

For some ions, such as chromium and halide ions, the values of ΔG^{cal}_{hyd} are particularly spread around the values calculated. The values of ΔG^{cal}_{hyd} depend on the R_{gmax}. The R_{gmax} of ions depend on the type of salt and H_20/salt molar ratio. Such as the R_{gmax} of Cr^{3+} are 1.90 from $CrCl_3$ with 110 H_20/salt molar ratio, and 2.03 from $Cr(NO_3)_3$ with 24.5–50.8 H_20/salt molar ratio{Ohtaki, 1993}.

5.6. Applying the strategies developed in this study to calculate the solvation free energy of multi-atom solutes such as proteins

For the solvation free energy of proteins, the R_{gmax} values of atoms were needed and can be estimated using MD simulations. Three layers of surface charges were constructed at the positions distant to solute atoms ($R_{gmax} + S(P_S)r_{M,O}$), ($R_{gmax} + S(P_S)r_{Hb,O}$) and ($R_{gmax} + R_W$). Each surface was divided into several hundreds of pieces, and the electric field on each piece, $-E_{net}$, was contributed by the partial charges of atoms in the solute, the surface charge on ($R_{gmax} + S(P_S)r_{M,O}$), ($R_{gmax} + S(P_S)r_{Hb,O}$), and ($R_{gmax} + R_W$). The surface charge density can also be calculated according to the net electric field on this surface. A numerical iteration method was used until the surface charge densities converged. In addition to the numerical method, because the generalized Born models are derived from Poisson's equation, they can be modified based on the strategies developed in this study.

6. Conclusion

In this study, we developed the strategy for calculating the solvation free energy that mimic the dielectric polarization surrounding the solute. The analytical solution describing the solvation free energy of ions were derived, yielding a physical basis for estimating the solvation free energy, and the source of error can be easily understood for comparing the trajectories of water molecules from MD simulations. The parameters used for calculating the solvation free energy, such as the TIP4P water model, the solvent molecular radius R_W and the solvent molecular polarizability γ_{mol}, were not obtained by fitting the experimental data of the solvation free energy.

Acknowledgments

We thank Professor Martin Karplus for the CHARMM program. This work was supported by Grant NSC100-2221-E-214-007-MY3 from the National Science Council of Taiwan.

References

[1] Y. Levy, J.N. Onuchic, Water mediation in protein folding and molecular recognition, Annu. Rev. Biophys. Biomol. Struct. 35 (2006) 389–415.
[2] M.K. Gilson, H.-X. Zhou, Calculation of protein-ligand binding affinities*, Annu. Rev. Biophys. Biomol. Struct. 36 (2007) 21–42.
[3] S. De Leeuw, J.W. Perram, E. Smith, Simulation of electrostatic systems in periodic boundary conditions. II. Equivalence of boundary conditions, Proc. R. Soc. Lond. A Math. Phys. Sci. 373 (1980) 57–66.
[4] D. Beglov, B. Roux, Finite representation of an infinite bulk system: solvent boundary potential for computer simulations, J. Chem. Phys. 100 (1994) 9050.
[5] P.-K. Yang, S.-H. Liaw, C. Lim, Representing an infinite solvent system with a rectangular finite system using image charges, J. Phys. Chem. B 106 (2002) 2973–2982.
[6] J.-P. Hansen, I.R. McDonald, Theory of Simple Liquids, 1990. (Access Online via Elsevier, 1990).
[7] J. Tomasi, Thirty years of continuum solvation chemistry: a review, and prospects for the near future, Theor. Chem. Accounts 112 (2004) 184–203.
[8] M. Born, Volumes and hydration warmth of ions, Zeitschrift Fur Physik 1 (1920) 45–48.
[9] M. Feig, W. Im, C.L. Brooks III, Implicit solvation based on generalized Born theory in different dielectric environments, J. Chem. Phys. 120 (2004) 903.
[10] M. Feig, A. Onufriev, M.S. Lee, W. Im, D.A. Case, C.L. Brooks, Performance comparison of generalized born and Poisson methods in the calculation of electrostatic solvation energies for protein structures, J. Comput. Chem. 25 (2004) 265–284.
[11] P.-K. Yang, C. Lim, The importance of excluded solvent volume effects in computing hydration free energies, J. Phys. Chem. B 112 (2008) 14863–14868.
[12] C.S. Babu, C. Lim, Solvation free energies of polar molecular solutes: application of the two-sphere Born radius in continuum models of solvation, J. Chem. Phys. 114 (2001) 889.
[13] R.M. Jackson, M.J. Sternberg, A continuum model for protein–protein interactions: application to the docking problem, J. Mol. Biol. 250 (1995) 258–275.

[14] I. Massova, P.A. Kollman, Combined molecular mechanical and continuum solvent approach (MM-PBSA/GBSA) to predict ligand binding, Perspect. Drug Discovery Des. 18 (2000) 113–135.
[15] R.C. Rizzo, T. Aynechi, D.A. Case, I.D. Kuntz, Estimation of absolute free energies of hydration using continuum methods: accuracy of partial charge models and optimization of nonpolar contributions, J. Chem. Theory Comput. 2 (2006) 128–139.
[16] R.M. Levy, L.Y. Zhang, E. Gallicchio, A.K. Felts, On the nonpolar hydration free energy of proteins: surface area and continuum solvent models for the solute-solvent interaction energy, J. Am. Chem. Soc. 125 (2003) 9523–9530.
[17] P.K. Yang, C. Lim, Strategies to model the near-solute solvent molecular density/polarization, J. Comput. Chem. 30 (2009) 700–709.
[18] P.K. Yang, Discrepancy in the near-solute electric dipole moment calculated from the electric field, J. Comput. Chem. 32 (2011) 2783–2799.
[19] P.-K. Yang, C. Lim, Reformulation of Maxwell's Equations to incorporate near-solute solvent structure, J. Phys. Chem. B 112 (2008) 10791–10794.
[20] P.-K. Yang, Derivation of equations describing distance solute oscillation of induced solvent polarization, Bull. Chem. Soc. Jpn. 84 (2011) 58–69.
[21] W.L. Jorgensen, J. Chandrasekhar, J.D. Madura, R.W. Impey, M.L. Klein, Comparison of simple potential functions for simulating liquid water, J. Chem. Phys. 79 (1983) 926.
[22] C. Lawrence, J. Skinner, Flexible TIP4P model for molecular dynamics simulation of liquid water, Z. Phys. 372 (2003) 842–847.
[23] J.D. Jackson, Classical Electrodynamics, 3rd ed. John Wiley & Sons, New York, 1999.
[24] B.R. Brooks, R.E. Bruccoleri, B.D. Olafson, S. Swaminathan, M. Karplus, CHARMM: a program for macromolecular energy, minimization, and dynamics calculations, J. Comput. Chem. 4 (1983) 187–217.
[25] J.-P. Ryckaert, G. Ciccotti, H.J. Berendsen, Numerical integration of the cartesian equations of motion of a system with constraints: molecular dynamics of n-alkanes, J. Comput. Phys. 23 (1977) 327–341.
[26] P.-K. Yang, C. Lim, Nonconvergence of the Solute Potential in an Infinite Solvent and Its Implications in Continuum Models, J. Phys. Chem. B 106 (2002) 12093–12096.
[27] H.S. Ashbaugh, R.H. Wood, Effects of long-range electrostatic potential truncation on the free energy of ionic hydration, J. Chem. Phys. 106 (1997) 8135.
[28] G. Hummer, L.R. Pratt, A.E. García, B.J. Berne, S.W. Rick, Electrostatic potentials and free energies of solvation of polar and charged molecules, J. Phys. Chem. B 101 (1997) 3017–3020.
[29] A. Narten, W. Thiessen, L. Blum, Atom pair distribution functions of liquid water at 25 °C from neutron diffraction, Science 217 (1982) 1033–1034.
[30] D.S. Cerutti, N.A. Baker, J.A. McCammon, Solvent reaction field potential inside an uncharged globular protein: a bridge between implicit and explicit solvent models? J. Chem. Phys. 127 (2007) 155101.
[31] C.S. Babu, C. Lim, Theory of ionic hydration: insights from molecular dynamics simulations and experiment, J. Phys. Chem. B 103 (1999) 7958–7968.
[32] Y. Marcus, Ionic radii in aqueous solutions, Chem. Rev. 88 (1988) 1475–1498.
[33] Y. Marcus, Thermodynamics of solvation of ions. Part 5.—Gibbs free energy of hydration at 298.15 K, J. Chem. Soc. Faraday Trans. 87 (1991) 2995–2999.
[34] H. Ohtaki, Ionic solvation in aqueous and nonaqueous solutions, Monatsh. Chem. 132 (2001) 1237–1268.
[35] H. Ohtaki, T. Radnai, Structure and dynamics of hydrated ions, Chem. Rev. 93 (1993) 1157–1204.